

# Computational Physics Project 2: Monte Carlo simulation of the two-dimensional XY model

Jan Masák, Eliisa Tökke

## Abstract

This project was done as a part of the Computational Physics course at Leiden University during the spring semester of the academic year 2024/2025. The goal of the project was to study the thermodynamic properties of the two-dimensional XY model. The simulation consisted of a  $60 \times 60$  lattice of spins with periodic boundary conditions. The properties of the system at different temperatures and external magnetic field values were studied with the Metropolis Monte Carlo algorithm. Our results agree well with theoretical predictions and previous studies and confirm that without external magnetic field the XY model undergoes a topological Kosterlitz-Thouless phase transition. When magnetic field is applied this transition disappears.

## 1 Introduction

The XY model imagines a 2D lattice  $\Lambda$  of sites  $i \in \Lambda$ , at each of which there is a vector  $\mathbf{s}_i \in \mathbb{S}^1$  on the unit circle (of unit length), which can be thought of as lying in the plane. This can be viewed as a generalisation of the Ising model because  $\mathbb{S}^0 = \{-1, 1\}$ . Each configuration is then represented by a set of spins  $\{\mathbf{s}_i\}_{i \in \Lambda}$  or, equivalently, through the parametrisation  $\mathbf{s}_i = (\cos \theta_i, \sin \theta_i)$  where  $\theta_i \in [-\pi, \pi)$ , by a set of angles  $\Theta = \{\theta_i\}_{i \in \Lambda}$ , which is the representation we will use most often. The simplest version then introduces interactions between the sites through the Hamiltonian

$$H[\Theta] = -J \sum_{\langle i, j \rangle} \mathbf{s}_i \cdot \mathbf{s}_j = -J \sum_{\langle i, j \rangle} \cos(\theta_i - \theta_j), \quad (1)$$

where  $J > 0$  is the coupling constant and  $\langle i, j \rangle$  denotes nearest neighbours. Because this Hamiltonian depends only on angle differences, it has the symmetry

$$H[\Theta] = H[\Theta + \Delta\theta] \quad \text{where} \quad \Delta\theta \in [-\pi, \pi), \quad (2)$$

which is a global U(1) symmetry. This is probably the most important difference from the Ising model, which also has a global symmetry, but a *discrete*  $\mathbb{Z}_2$  symmetry. Because of this continuous symmetry, we have the Mermin–Wagner theorem [6], which states that in a system with such local interactions, continuous symmetries cannot be spontaneously broken at finite temperature when the spatial dimension is  $\leq 2$ . This means that the system cannot have the ordered, magnetised phase we observe, for example, in the 2D Ising model, which is a classic example of spontaneous symmetry ( $\mathbb{Z}_2$ ) breaking. It also implies that the system cannot develop a non-zero mean magnetisation, which would normally serve as our order parameter.

The physical process behind the impossibility of spontaneous magnetisation is the existence of long-wavelength (low-energy) spin waves [10]. Deviations from order can then be quantified by the momentum-space integral

$$\int \frac{d^2 k}{k^2}. \quad (3)$$

If we take our lattice to be  $N \times N$ , this integral scales as  $\ln N$ , leading to an infrared divergence in the thermodynamic limit. However, since this divergence is slow and in our simulation the lattice is finite and small, as we will see, the system still develops a non-zero magnetisation at low temperatures.

As already mentioned, in the thermodynamic limit the mean magnetisation vanishes and we have no local order parameter. This prevents the system from exhibiting a standard phase transition in Landau's paradigm, which classifies phase transitions based on discontinuities in derivatives of an order parameter.

Does this mean that there is no phase transition in the 2D XY model? Actually, as we will see from the results of our simulation, there still appears to be a point exhibiting properties characteristic of a phase transition, such as a divergent magnetic susceptibility. However, it is a different kind of phase transition, first described by Kosterlitz and Thouless (KT) [5] — a topological phase transition.

The discovery and study of this novel kind of phase transition earned KT the 2016 Nobel Prize in Physics. This transition is considered topological because it can be studied through the behaviour of topological defects - vortices, which we also observe in our simulation. The XY model can be regarded as the simplest model exhibiting this kind of phase transition, but at the same time it is not fully analytically solvable. It has therefore been thoroughly studied since the 1970s [4] and remains an active area of research. Thus it is also a perfect playground for exploring the KT phase transition through computer simulations.

In our work, we also discuss the effect of an external magnetic field, corresponding to the Hamiltonian

$$H[\Theta] = -J \sum_{\langle i,j \rangle} \mathbf{s}_i \cdot \mathbf{s}_j - \mathbf{h} \cdot \sum_{i \in \Lambda} \mathbf{s}_i = -J \sum_{\langle i,j \rangle} \cos(\theta_i - \theta_j) - h \sum_{i \in \Lambda} \cos \theta_i, \quad (4)$$

where  $h = |\mathbf{h}|$  is the magnitude of the field. This is a significant perturbation since it breaks the global  $U(1)$  symmetry of the original theory. As mentioned in [3] any magnetic field causes the KT phase transition to disappear as it happens in the 2D Ising model (because the  $\mathbb{Z}_2$  symmetry is no longer broken spontaneously but explicitly). We observe this in our simulation.

## 2 Methods

### 2.1 Monte Carlo integration and the Metropolis algorithm

The Monte Carlo method is a powerful approach for studying the properties of a system at equilibrium, if we are not interested in its dynamics, and need to calculate high-dimensional integrals. In statistical physics, we typically have to evaluate integrals of the form

$$\langle A \rangle = \int_M \mathcal{D}\Theta \frac{e^{-\beta H[\Theta]}}{Z} A[\Theta], \quad \text{where} \quad Z = \int_M \mathcal{D}\Theta e^{-\beta H[\Theta]}, \quad (5)$$

with  $\mathcal{D}\Theta = \prod_{i \in \Lambda} d\theta_i$  and  $M = [-\pi, \pi)^{N^2}$  which can be thought of as the configuration space of the system. We therefore see that we have a very high-dimensional integral ( $N^2$  dimensional), that can be evaluated with the Monte Carlo method, but additional complexity arises from the fact that the function  $A[\Theta]e^{-\beta H[\Theta]}$  is usually very sharply peaked. This requires that we do not sample over the configuration space with the uniform distribution like the simplest Monte Carlo method does, but it demands the use of importance sampling.

Importance sampling can be implemented by means of the Metropolis algorithm [7]. This algorithm is also nice because it assumes that we know the target distribution just up to a normalisation factor. This is exactly the case with the Boltzmann distribution  $\pi[\Theta(t)] = e^{-\beta H[\Theta]}/Z$  because we do not know the partition function  $Z$ . Metropolis algorithm can be well understood using the concept of a Markov chain: a set of random states  $\Theta(t)$ , where the probability of  $\Theta(t+1)$  depends only on  $\Theta(t)$ . A Markov chain is fully described by transition probabilities  $T(\Theta \rightarrow \Theta')$  such that

$$\int_M \mathcal{D}\Theta' T(\Theta \rightarrow \Theta') = 1. \quad (6)$$

In the Metropolis algorithm, one divides these probabilities as

$$T(\Theta \rightarrow \Theta') = w(\Theta'|\Theta) \times A(\Theta'|\Theta). \quad (7)$$

The first factor  $w(\Theta'|\Theta)$  denotes the probability to propose a new state  $\Theta'$  given a state  $\Theta$ , and the second factor  $A(\Theta'|\Theta)$  denotes the probability to accept the proposed new state  $\Theta'$  if the system was before in the state  $\Theta$ . Transition probabilities uniquely define a Markov process. To ensure that a Markov process has a unique stationary distribution, two conditions must be met [9]:

**1. Existence of a stationary distribution:**

A sufficient (though not necessary) condition for the existence of a stationary distribution  $\pi[\Theta]$  is the *detailed balance* condition:

$$\pi[\Theta] T(\Theta \rightarrow \Theta') = \pi[\Theta'] T(\Theta' \rightarrow \Theta)$$

This condition is commonly satisfied in systems at thermodynamic equilibrium.

**2. Uniqueness of the stationary distribution:**

This is guaranteed by *ergodicity* of the Markov chain, a property commonly assumed in the Metropolis algorithm [7]. A key component of ergodicity is *irreducibility*, which ensures that the Markov chain can explore the entire configuration space over time. As we shall see, in our system, this assumption may break down at low temperatures due to finite-size effects, casting doubt on the validity of our results in that regime.

If we assume that  $w$  is symmetric (i.e.  $w(\Theta'|\Theta) = w(\Theta|\Theta')$ ) as the Metropolis algorithm does, the detailed balance condition can be written as

$$\frac{A(\Theta'|\Theta)}{A(\Theta|\Theta')} = \frac{\pi[\Theta']}{\pi[\Theta]}, \quad (8)$$

which can be satisfied with

$$A(\Theta'|\Theta) = \begin{cases} 1 & \text{if } \pi[\Theta'] > \pi[\Theta], \\ \pi[\Theta']/\pi[\Theta] & \text{if } \pi[\Theta'] < \pi[\Theta]. \end{cases} \quad (9)$$

The Metropolis algorithm thus consists of the following steps:

1. Start with a random initial state  $\Theta(0)$ .
2. Generate a state  $\Theta'$  from  $\Theta(t)$ .
3. If  $\pi(\Theta') > \pi[\Theta(t)]$ , then  $A(\Theta'|\Theta) = 1$  and set  $\Theta(t+1) = \Theta'$ . Otherwise, accept move with probability  $p = \pi[\Theta']/\pi[\Theta(t)]$ .
4. Continue with (2).

In our case,  $\pi[\Theta(t)]$  is the Boltzmann distribution  $\pi[\Theta(t)] = e^{-\beta H[\Theta]}/Z$ . Thus, the trial move that lowers the energy is always accepted, and a move that increases the energy by an amount  $\Delta E = H[\Theta'] - H[\Theta]$  is accepted with a probability  $e^{-\beta \Delta E}$ . This means that the system will try to move towards lower total energy, but the higher the temperature, the higher is the probability to flip a spin and go to a state with more energy.

For practical implementation, we chose the trial step probabilities to be

$$w(\Theta'|\Theta) = \begin{cases} 1/N^2 & \text{if } \Theta \text{ and } \Theta' \text{ differ by one spin;} \\ 0 & \text{otherwise.} \end{cases} \quad (10)$$

This means that when spins are in state  $\Theta$ , we create a trial state  $\Theta'$  by picking one spin at random and changing its angle by a random increment  $[-\Delta, \Delta] \subset [-\pi, \pi]$ . This increment we choose in our simulation such that the average acceptance probability is close to 0.5 to efficiently explore the space of possibilities. After that we calculate the energy difference  $\Delta E$  by computing the change in the interaction energy of the picked spin with its four neighbours. We always accept the move if  $\Delta E < 0$ , and if  $\Delta E > 0$ , we accept the move with a probability  $e^{-\beta \Delta E}$ .

## 2.2 Initial conditions

We used a square grid of  $60 \times 60$  spins with periodic boundary conditions and the coupling constant  $J$  set to 1. For  $h = 0$ , we ran the simulation from temperature  $T = 0.5$  to  $T = 2.5$ , with an increment of 0.2 (in units where  $J = k_B = 1$ ). We also picked two additional points close to the critical temperature, at  $T = 0.8$  and  $T = 0.87$ . We expect the critical point for  $h = 0$  to be around  $T_C = 0.89$  [10, 2]. After receiving results for  $h = 0$ , we turned on the external magnetic field and used two different field strengths ( $h = 0.05$  and  $h = 0.4$ ) to see the effect it has on the behaviour of the system. With  $h \neq 0$ , we used fewer temperatures and concentrated mainly on regions that we expected to be interesting based on the work done by Jensen and Weber [3].

### 2.3 Equilibrating the system

We were interested in the properties of the system at equilibrium, therefore it was necessary at each temperature to find the equilibration time of the system and let the system reach equilibrium before starting the measurements. We found the equilibration time by inspecting the magnetization curves at different temperatures. An example of such a curve is shown in figure 1. Based on that curve, we estimated the equilibration time at  $T = 0.5$  (without external magnetic field) to be 500 sweeps.

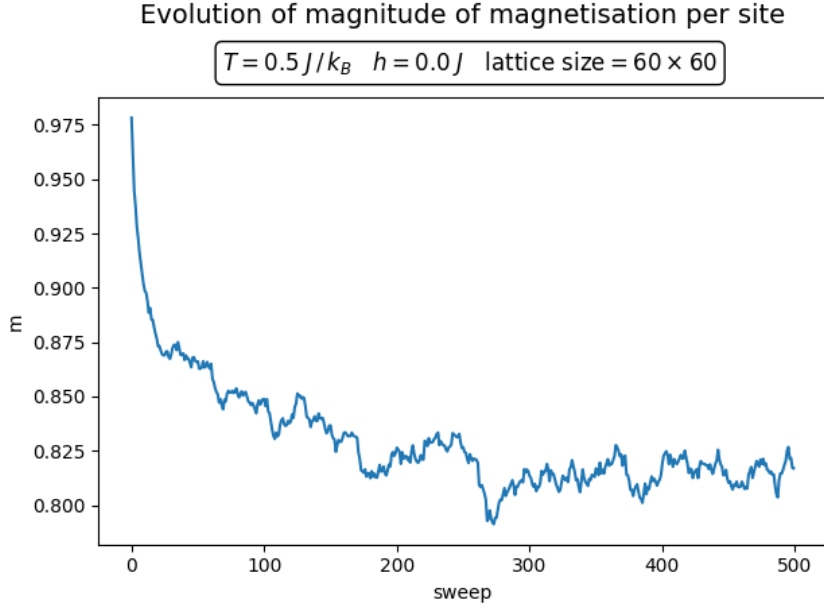


Figure 1: Evolution of magnitude of magnetization per site at  $T = 0.5$ .

For each temperature, we also found whether it is more efficient to start from a cold (all spins aligned) or hot (all spins random) configuration. The results are presented in table 1. Having a non-zero external magnetic field significantly reduced the time required for equilibration. This can be explained by the field breaking the global  $U(1)$  symmetry, forcing spins to align in the direction of the field, thus restricting random fluctuations and shortening the time needed for the system to settle.

Table 1: Equilibration Data by Temperature

Temperature	$h = 0$		$h = 0.05$		$h = 0.4$	
	Eq. time	Best start	Eq. time	Best start	Eq. time	Best start
0.5	500	cold				
0.7	1000	cold	500	cold	250	cold
0.8	1000	cold	500	cold		
0.87	1500	cold				
0.9	1000	cold	250	cold	250	cold
1.1	750	hot	250	cold	250	cold
1.3	750	hot	500	hot	250	cold
1.4					250	cold
1.5	500	hot	250	hot	250	cold
1.7	250	hot	250	hot	250	cold
1.9	250	hot				
2.1	250	hot				
2.3	250	hot				
2.5	250	hot				

## 2.4 Measured quantities

The following is an overview of the quantities that were measured in the simulation. But first, a few remarks about notation: we denote the total magnetisation  $\mathbf{M} = \sum_{i \in \Lambda} \mathbf{s}_i$ . The total magnetisation per spin is then  $\mathbf{m} = \mathbf{M}/N^2$ . Vector norms are always denoted just  $M = |\mathbf{M}|$  and  $m = |\mathbf{m}|$ . The time averages that should converge into ensemble averages are denoted as

$$\langle A \rangle = \frac{1}{T} \sum_{t=1}^T A(t) \quad \text{and} \quad \langle A(t) \rangle = \frac{1}{T} \sum_{t'=1}^T A(t' + t). \quad (11)$$

One of the simulation's outputs is the average magnitude of total magnetization per spin:  $\langle m \rangle = \langle M \rangle / N^2$ . Another option would be to measure  $\langle \mathbf{m} \rangle$ , which should be 0 if  $h = 0$ , but in reality it is unstable at low temperatures. Below the critical temperature, the system acquires a magnetization and it would take a very long time for it to reach zero [8]. Because of this,  $\langle \mathbf{m} \rangle$  is not a stable quantity and it is more useful to measure  $\langle m \rangle$ . Analogously to magnetization, the energy per spin is measured as  $e = E/N^2$ , where  $E$  is the total energy of the system.

The standard deviation of magnetization (and analogously of energy) is calculated as

$$\sigma = \sqrt{\frac{2\tau}{t_{\max}} \left( \langle m^2 \rangle - \langle m \rangle^2 \right)}, \quad (12)$$

where  $\tau$  is the autocorrelation time - the time it takes for the system to forget it's previous state. Autocorrelation time is calculated from the autocorrelation function:

$$\chi(t) = \langle \mathbf{m} \cdot \mathbf{m}(t) \rangle - \langle \mathbf{m} \rangle \cdot \langle \mathbf{m}(t) \rangle. \quad (13)$$

The autocorrelation function should decay as  $\chi(t) \sim e^{-t/\tau}$ . In our simulation we approximate  $\tau$  as

$$\sum_{t=0}^{t_{\max}} \frac{\chi(t)}{\chi(0)} \simeq \sum_{t=0}^{t_{\max}} e^{-t/\tau} \sim \int_0^{\infty} e^{-t/\tau} dt = \tau, \quad (14)$$

where the last approximation holds for large  $t_{\max}$ . So in our simulation we approximate the autocorrelation time using this sum and choosing  $t_{\max}$  so that the summation stops once  $\chi(t) < 0$ , which signals the onset of poor statistics. Figures 2a and 2b display example measurements of the autocorrelation function at  $T = 0.7$  and  $T = 1.1$ . We can see that if the temperature is high (figure 2b), the autocorrelation function follows the exponential approximation quite accurately (in the beginning while  $\chi(t) > 0$ ). But at low temperatures (figure 2a) we observe slower decay and the difference between the exponential fit and actual values is significant. This confirms our worry expressed in in section 2.1 that at low temperatures the systems does not have the opportunity to explore properly the configuration space. This is probably because of it finite size it picks up a magnetisation around which it gets stuck.

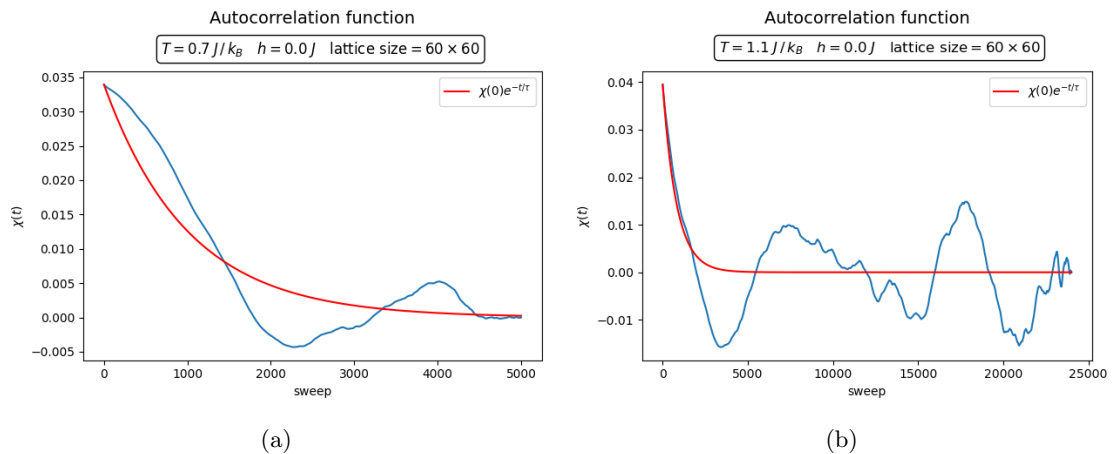


Figure 2: Autocorrelation functions at temperatures  $T = 0.7$  and  $T = 1.1$  with  $h = 0$ .

Additional quantities measured in the simulation are magnetic susceptibility per spin

$$\chi_M = \frac{1}{N^2 k_B T} (\langle \mathbf{M} \cdot \mathbf{M} \rangle - \langle \mathbf{M} \rangle \cdot \langle \mathbf{M} \rangle) \quad (15)$$

and specific heat per spin:

$$C = \frac{1}{N^2 k_B T^2} (\langle E^2 \rangle - \langle E \rangle^2). \quad (16)$$

Magnetic susceptibility and specific heat per spin are measured in the following way: the simulation is divided into successive blocks, each containing  $n$  measurements. For each block,  $\chi_M$  and  $C$  are determined, and the standard error is estimated based on the blocks. The length of the blocks is set to  $16\tau$ . This means that close to the critical point, the simulation takes longer because the autocorrelation time is larger close to the critical point.

An interesting feature that appears in the XY model at low temperatures are pairs of vortices and antivortices. Figure 3 displays the last state of a simulation run at  $T = 0.9$  with vortex-antivortex pairs. To quantify this phenomenon, the simulation measures the average vortex pair density and plots the distribution of vortex pair member distances. The presence of bound vortex pairs in the low-temperature phase, and the pairs unbinding in the high-temperature phase, is one of the main aspects of the KT theory [10].

The vortices are found by moving around a closed loop of four neighbouring spins and calculating the change in the spins along the path. The net change in spin direction will be  $2\pi$  times an integer if there is a single vortex of unit strength in the loop. This integer can be greater than one only if the four spins in the loop have relative angles of  $\pi$ ,  $-\pi$ ,  $\pi$  and  $-\pi$ . The probability for this to occur is negligible, thus we only need to consider vortices of unit strength [10].

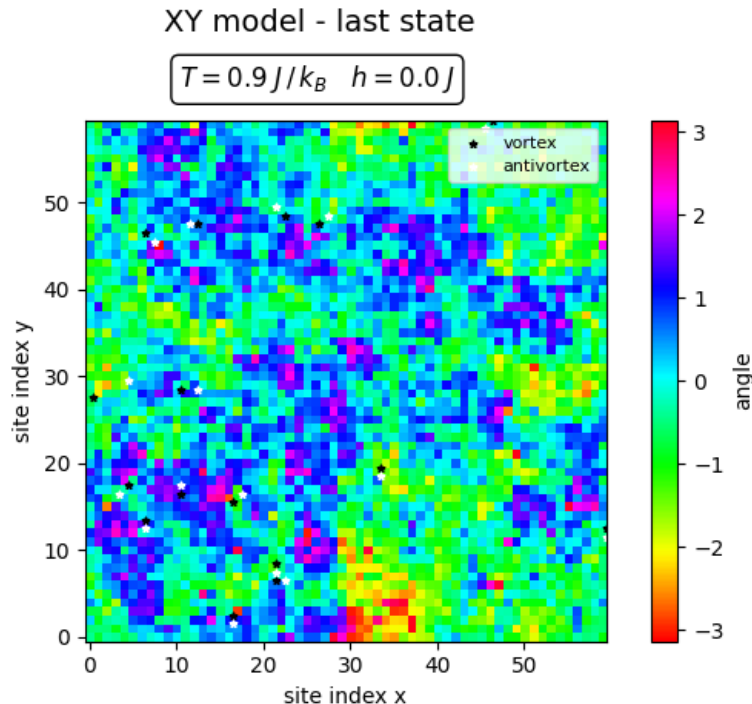


Figure 3: The two-dimensional XY model at  $T = 0.9$  and  $h = 0$ , in a state with pairwise bound vortices.

### 3 Results and discussion

Figure 4 displays autocorrelation times at each temperature and magnetic field strength. We can notice several interesting phenomena from the plot. Without an external magnetic field, we can clearly see the

existence of a critical point around  $T_C \approx 0.9$ . Autocorrelation time diverges around the critical point, as expected from the KT phase transition theory [4]. At low temperature the autocorrelation time is not properly defined - its value differs between runs. This arises due to the finite size effects already discussed. To keep the simulation run-time reasonable at these temperatures, we assigned the autocorrelation times by hand with a maximum of  $\tau = 200$ , even if the measured value was larger.

At temperatures larger than critical, the autocorrelation time stabilizes. The plot also displays the effect of external magnetic fields - even in the case of a weak field ( $h = 0.05$ ), the autocorrelation time does not diverge any more at the critical point. Although the values of the autocorrelation time are still larger at low temperatures, they are confined to a reasonable range. Strong magnetic field ( $h = 0.4$ ) dramatically decreases the autocorrelation time.

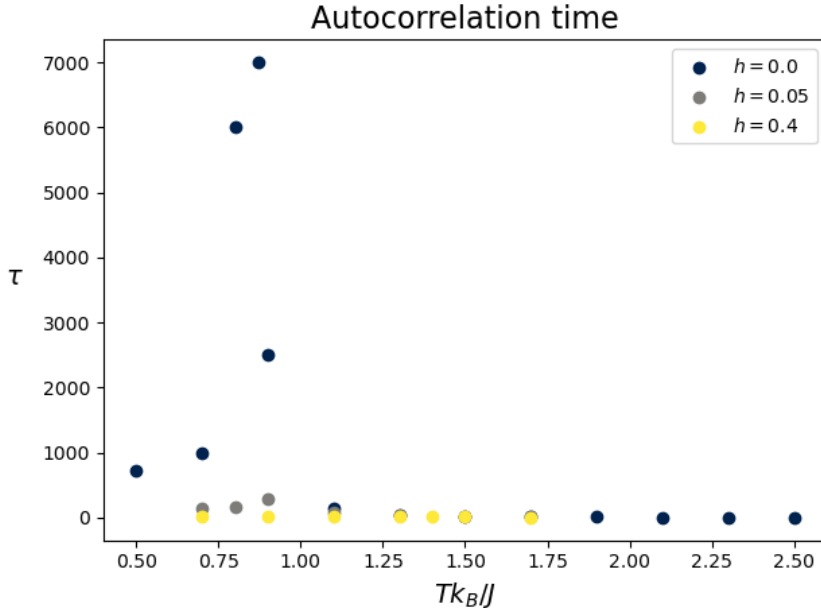


Figure 4: Autocorrelation time as a function of temperature

Figure 5a shows the mean magnetization magnitude per spin. In the case without an external magnetic field, it is interesting to note the sharp decrease in magnetization magnitude after the critical point. At high temperatures, the mean magnetization magnitude is approximately zero. This behaviour agrees with the results found in [8] (Fig. 4). As expected, the magnetization is stronger in systems where  $h \neq 0$ . With a weak magnetic field, the dependence of the mean magnetization magnitude on temperature is qualitatively similar to  $h = 0$ , but shifted towards higher temperatures. With a strong magnetic field ( $h = 0.4$ ), the sharp decrease disappears.

Figure 5b displays the relation between temperature and mean energy per spin. It is in very good agreement with results found in the literature (Fig. 3 in [8], Table 2 and Fig. 4 in [10], and Table 1 in [1]). At temperatures relatively low compared to the external magnetic field the absolute value of the energy of the system, the reason for which is clear from the XY model's Hamiltonian.

The relation between temperature and specific heat per spin is shown in figure 5c. Specific heat exhibits a peak around the critical point. The reason for this is that Kosterlitz-Thouless phase transition is characterized by vortex-antivortex pair formation. Close to the transition, these pairs unbind, creating strong fluctuations, which significantly impact the heat capacity. Our results are in good agreement with those found in Fig. 2 in [8], Fig. 5 in [10], Table 1 in [1] and Fig. 3 in [3].

Adding an external magnetic field flattens the peak and shifts it to higher temperatures. This happens because the external field aligns spins more strongly in a preferred direction, which reduces fluctuations in the system. Since the specific heat measures how much energy is absorbed per unit temperature change, less fluctuations means a more gradual change in energy and thus a flattened curve.

Magnetic susceptibility per spin exhibits interesting behaviour in figure 5d. Without an external magnetic field, it quickly reaches zero above the critical temperature. But below the critical temperature it is not clearly defined - the uncertainties get very large. The general behaviour of magnetic susceptibility agrees with Fig. 1 in [8]. Other sources also report the large increase of magnetic susceptibility close and below the critical temperature (Table 1 and Fig. 3 in [10], Table 1 and Fig. 2 in [2], Table 1 in [1]). Magnetic susceptibility is high at low temperatures because spins tend to align coherently over large distances. When an external magnetic field is applied, the system responds strongly because the spins are already correlated, leading to high magnetic susceptibility. Also, at low temperatures, excitations are dominated by low-energy spin waves rather than random fluctuations. These waves can be easily influenced by an external field which increases the system's susceptibility. Adding an external magnetic field increases the magnetic susceptibility, and also makes it stable even at low temperatures.

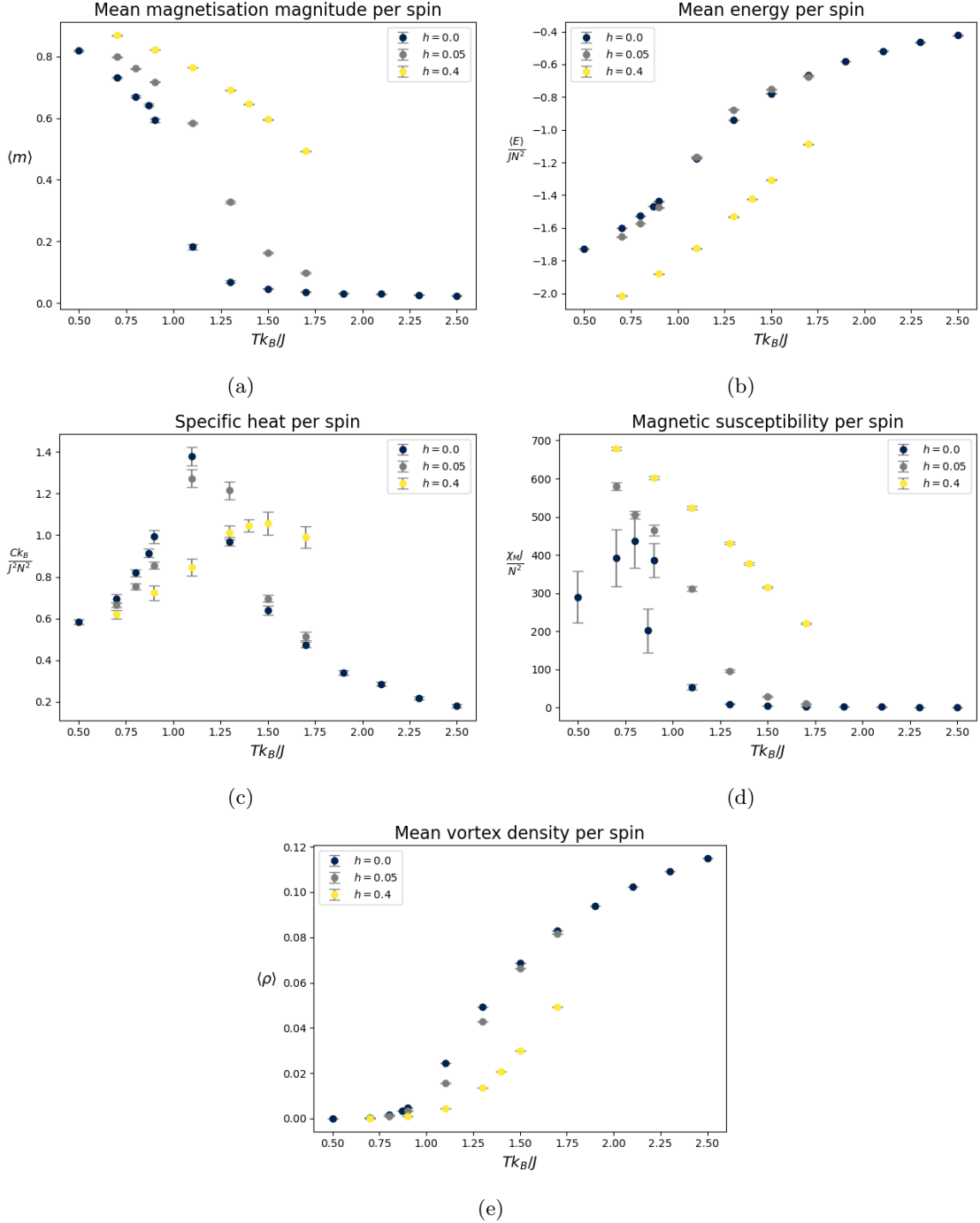


Figure 5: Physical quantities measured in the simulation.

Figure 5e shows the relation between temperature and mean vortex density per spin. The number of vortices increases rapidly at temperatures higher than the critical temperature. As mentioned in the introduction, this is a sign of topological phase transition. Our results are in good agreement with those presented in Fig 2. in [3]. The number of vortices at a certain temperature is relatively stable, but not conserved. This is because spins still fluctuate, which enables spontaneous vortex creation and annihilation.

Vortex pair member distance distributions at low ( $T = 0.7$ ) and high ( $T = 2.0$ ) temperatures with  $h = 0$  are shown as histograms in figures 6a and 6b, respectively. These figures illustrate that at low temperatures there are few vortices and they are pairwise bound (their distance is mostly of one site). At high temperatures we observe that the distribution of distances is broader signifying unbinding of the vortices. This further confirms that the system undergoes a topological phase transition. Unfortunately, our histograms were not accurate enough to pinpoint the value of the critical temperature. This can be, might be, for example, because of the small size of our simulation or because we used a greedy algorithm to match vortices into pairs.

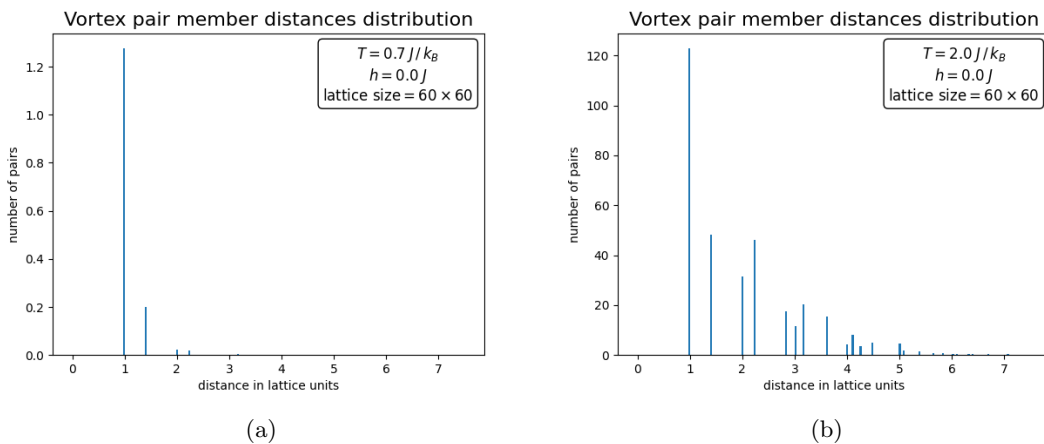


Figure 6: Histograms of vortex pair member distances distributions at low ( $T = 0.7$ ) and high ( $T = 2.0$ ) temperatures.

Based on the figures presented in this section, we can conclude that external magnetic fields effectively remove the topological phase transition, but the system still exhibits some critical behaviour. Interesting thing to note is that if the magnetic field strength increases, the critical temperature of the system also increases - points on the plots are shifted to the right.

## 4 Conclusion

This Monte Carlo simulation of the two-dimensional XY model successfully captured the properties and behaviour of the system, as expected from theoretical predictions and previous studies. Our results confirmed the presence of the topological Kosterlitz-Thouless phase transition, as evidenced by the divergence of both autocorrelation time and magnetic susceptibility and the rapid increase in vortex density above the critical temperature. The simulation also demonstrated the strong impact external magnetic fields have on the XY model: even a weak magnetic field significantly decreases both equilibration and autocorrelation times and makes the system more stable at low temperatures. External magnetic fields effectively remove the topological phase transition, but the system still exhibits some critical behaviour.

This simulation demonstrates the power of the Monte Carlo method for studying complex statistical physics phenomena, because we received accurate results even with a relatively small lattice and manually assigned autocorrelation times at low temperatures. The simulation could be developed further by using larger lattice sizes to analyze the model's behaviour around the critical temperature in more detail and eliminate finite-size effects. Additionally, studying non-equilibrium vortex dynamics or extending the analysis to anisotropic modifications of the XY model would provide interesting insights into the effects of external perturbations on topological transitions.

## References

- [1] Rajan Gupta and Clive F Baillie. “Critical behavior of the two-dimensional XY model”. In: *Physical Review B* 45.6 (1992), p. 2883.
- [2] Rajan Gupta et al. “Phase Transition in the 2D XY Model”. en. In: *Physical Review Letters* 61.17 (Oct. 1988), pp. 1996–1999. ISSN: 0031-9007. DOI: [10.1103/PhysRevLett.61.1996](https://doi.org/10.1103/PhysRevLett.61.1996).
- [3] Henrik Jeldtoft Jensen and Hans Weber. “Phenomenological study of vortices in a two-dimensional XY model in a magnetic field”. en. In: *Physical Review B* 45.18 (May 1992), pp. 10468–10472. ISSN: 0163-1829, 1095-3795. DOI: [10.1103/PhysRevB.45.10468](https://doi.org/10.1103/PhysRevB.45.10468).
- [4] J Michael Kosterlitz. “The critical properties of the two-dimensional xy model”. In: *Journal of Physics C: Solid State Physics* 7.6 (1974), p. 1046.
- [5] John Michael Kosterlitz and David James Thouless. “Ordering, metastability and phase transitions in two-dimensional systems”. In: *Journal of Physics C: Solid State Physics* 6.7 (1973), p. 1181.
- [6] N David Mermin and Herbert Wagner. “Absence of ferromagnetism or antiferromagnetism in one-or two-dimensional isotropic Heisenberg models”. In: *Physical Review Letters* 17.22 (1966), p. 1133.
- [7] Nicholas Metropolis et al. “Equation of State Calculations by Fast Computing Machines”. en. In: *Journal of Chemical Physics* 21.6 (June 1953), pp. 1087–1092. ISSN: 0021-9606. DOI: [10.1063/1.1699114](https://doi.org/10.1063/1.1699114).
- [8] Seiji Miyashita et al. “Monte Carlo Simulation and Static and Dynamic Critical Behavior of the Plane Rotator Model”. In: *Progress of Theoretical Physics* 60.6 (Dec. 1978), pp. 1669–1685. ISSN: 0033-068X. DOI: [10.1143/PTP.60.1669](https://doi.org/10.1143/PTP.60.1669).
- [9] Christian P. Robert and George Casella. *Monte Carlo Statistical Methods*. eng. New York, NY : Springer New York, 2004. ISBN: 978-1-4757-4145-2.
- [10] Jan Tobochnik and G. V. Chester. “Monte Carlo study of the planar spin model”. en. In: *Physical Review B* 20.9 (Nov. 1979), pp. 3761–3769. ISSN: 0163-1829. DOI: [10.1103/PhysRevB.20.3761](https://doi.org/10.1103/PhysRevB.20.3761).